



## DFT calculation for stability and strength of iron borides

H.H. Huang<sup>a</sup>, Xiaofeng Fan<sup>a,\*</sup>, G.M. Yang<sup>a,d</sup>, David J. Singh<sup>c</sup>, W.T. Zheng<sup>a,b</sup>

<sup>a</sup> Key Laboratory of Automobile Materials (Jilin University), Ministry of Education, and College of Materials Science and Engineering, Jilin University, Changchun 130012, China

<sup>b</sup> State Key Laboratory of Superhard Materials, Jilin University, Changchun 130012, China

<sup>c</sup> Department of Physics and Astronomy, University of Missouri, Columbia, MO 65211-7010, USA

<sup>d</sup> College of Physics, Changchun Normal University, Changchun 130032, China



### ARTICLE INFO

#### Article history:

Received 1 November 2017

Received in revised form 12 December 2017

Accepted 14 December 2017

#### Keywords:

First-principles methods

Superhard materials

Hardness

Stress-strain curves

Ideal strength

### ABSTRACT

The structural stability and mechanical properties of  $\text{FeB}_x$  have been investigated by first principles methods with semiempirical model. With the analysis of the mechanical properties in both elastic and plastic regions, it is found that the hardness of  $\text{FeB}_x$  becomes higher by following the increase of B content up to  $\text{FeB}_2$ . From the stress-strain curves with the semiempirical model about hardness, the hardness of  $\text{FeB}_2$  is about 31 GPa and similar to that of  $\text{FeB}_4$ . It is expected that these results can give some light on the applications of  $\text{FeB}_x$  with high B content, such as the boronizing of iron surface.

© 2017 Elsevier B.V. All rights reserved.

### 1. Introduction

Superhard materials are of tremendous interest in both technological applications and fundamental science. Due to the superior mechanical and physical property, they can be used in a variety of industrial applications such as cutting tools, hard coatings, and abrasives and are synthesized by the design [1–4]. Among the superhard materials, the borides are expected to have the excellent properties [5,6]. For example, boron can combine with other light elements, such as C and N to form the superhard alloys  $\text{BC}_5$  [7–9],  $\text{BC}_3$  [10–12],  $\text{BC}_2\text{N}$  [13–15], and so on. These materials with the strong covalent bond network have fine mechanical properties. However, their preparation condition is harsh and the increased production costs prevent them from being used in industry [6]. Recently, another category of borides with the combination of boron and transition metals, such as Cr, Re, W, Os, Fe, etc were found to have the ultra-incompressible and expected to have good mechanical properties [6,16–24]. For example,  $\text{ReB}_2$  was synthesized under ambient pressure and with a hardness of 48 GPa [16], which was comparable to that of cubic BN [25].  $\text{OsB}_2$  was shown to have an ultra-incompressible hard behavior [6]. The strength of  $\text{WB}_4$  was reported to reach up to 46 GPa [17,18]. In addition to high hardness, these borides also possibly exhibit superior

electronic properties, such as the typical superconductive  $\text{MgB}_2$  with a  $T_c$  of 39 K [19].

With the structure search, iron-based borides  $\text{FeB}_4$  ( $\text{op10-FeB}_4$ ) were considered to thermodynamically stable and predicted to have the phonon-mediated superconducting characteristic, recently [26]. Subsequently, the route for the  $\text{FeB}_4$  synthesis with pressure was suggested [27] and it was synthesized experimentally at a pressure above 8 GPa and high temperature by Gou et al. [28]. The results of magnetic susceptibility and heat capacity demonstrated the superconductivity below 2.9 K. In addition, it was found that the new phase  $\text{FeB}_4$  had the highly incompressible with a nanoindentation hardness of about 62 GPa [28]. The reported anomalous high hardness more than 60 GPa is considered to be a strong deviation from that of the well-known transition metal borides. The stability of  $\text{FeB}_4$  with different crystal structure was studied [29] and the hardness derived by the semiempirical method was shown to be lower than the experimental result, not exceeding the superhard threshold of 40 GPa. Moreover, Li et al. [30] investigated the ideal strength of  $\text{FeB}_4$  using first principles methods to analyze the contribution of the stress response. The stress-strain relations under different loading conditions showed the indentation strength of  $\text{FeB}_4$  was about 17 GPa [30] and its Vickers hardness was estimated to be about 25 GPa [31]. As we know, the detailed understanding of the stability and mechanical properties of Fe–B alloy system is still limited, though that of  $\text{FeB}_4$  may be analyzed well [32–36].

\* Corresponding author.

E-mail address: [xffan@jlu.edu.cn](mailto:xffan@jlu.edu.cn) (X. Fan).

In this work, we investigated the structural stability and mechanical properties of Fe-B alloy by considering the different phases including Fe<sub>2</sub>B and FeB from the previous Fe-B phase diagram, and both FeB<sub>2</sub> and FeB<sub>4</sub> from the structural research with first-principles methods. By following the change of B content, the relative stability of these structures under pressure was analyzed by considering the formation enthalpy. With the calculations of elastic constants and the analysis of shear stress-strain relations, the mechanical properties of FeB<sub>x</sub> with different B contents were explored. The charge distribution in real space was analyzed in order to get a deep insight into the tendency in mechanical strength with the content of boron in the Fe-B compounds.

## 2. Computational method

We carried out the first-principle calculations with the accurate frozen-core full-potential projector augmented wave (PAW) method as implemented in the Vienna ab initio simulation package (VASP) [37,38]. The calculations performed were based on density functional theory with the exchange and correlation effects described by the generalized gradient approximation (GGA) of Perdew, Burke, and Ernzerhof (PBE) [39]. A plane wave basis with an energy cutoff of 500 eV was used. The Monkhorst-Pack grid [40] with a k-point spacing of 0.02 Å were chosen in the Brillouin zone for the total energy convergence at the 1 meV/atom level. The energy convergence criterion was 10<sup>-6</sup> eV and the Hellmann-Feynman forces were relaxed to below 0.01 eV Å<sup>-1</sup>. The spin-polarization effect is considered due to the partial occupations of 3d-orbitals of Fe. In addition, to consider the strong correlations from 3d<sub>Fe</sub>, the GGA + U was tested and the Hubbard parameter U didn't result in the obvious effect on mechanical properties of Fe<sub>x</sub>B.

From the structural research about binary alloy FeB<sub>x</sub> [26], there are four possible single-phases for the different contents of B including x = 0.5, 1, 2 and 4. For the four phases Fe<sub>2</sub>B, FeB, FeB<sub>2</sub> and FeB<sub>4</sub> (op10-FeB<sub>4</sub>), the corresponding possible stable structures are with space groups *I4/mcm*, *Pnma*, *Pnma*, and *Pnmm* [26], respectively. In addition, the energy-favorable structure (tp10-FeB<sub>4</sub>) of FeB<sub>4</sub> under high pressure is found to be with *P42/nmc*. These structures are plotted in Fig. 1.

The elastic constants were obtained by calculating the stress under small special strain with first-principles methods. For tetragonal phases, the bulk modulus and shear modulus with the Voigt model can be expressed by the equation [42],

$$B_V = (1/9)[2(C_{11} + C_{12}) + C_{33} + 4C_{13}], \text{ and } G_V = (1/30)(M + 3C_{11} - 3C_{12} + 12C_{44} + 6C_{66}).$$

For the Reuss model, they are expressed as,

$$B_R = C^2/M \text{ and } G_R = 15 \left\{ (18B_V/C^2) + [6/(C_{11} - C_{12})] + (6/C_{44}) + (3/C_{66}) \right\}^{-1}.$$

In these formulas, M and C<sup>2</sup> are denoted by,

$$M = C_{11} + C_{12} + 2C_{33} - 4C_{13}, \text{ and } C^2 = (C_{11} + C_{12})C_{33} - 2C_{13}^2.$$

For orthorhombic phases, the bulk and shear modulus with the Voigt model can be expressed by the equation,

$$B_V = (1/9)[C_{11} + C_{22} + C_{33} + 2(C_{12} + C_{13} + C_{23})], \text{ and}$$

$$G_V = (1/15)[C_{11} + C_{22} + C_{33} + 3(C_{44} + C_{55} + C_{66}) - (C_{12} + C_{13} + C_{23})].$$

For the Reuss approximation, they are expressed as,

$$B_R = \Delta [C_{11}(C_{22} + C_{33} - 2C_{23}) + C_{22}(C_{33} - 2C_{13}) - 2C_{33}C_{12} + C_{12}(2C_{23} - C_{12}) + C_{13}(2C_{12} - C_{13}) + C_{23}(2C_{13} - C_{23})]^{-1}, \text{ and}$$

$$G_R = 15 \{ 4[C_{11}(C_{22} + C_{33} + C_{23}) + C_{22}(C_{33} + C_{13}) + C_{33}C_{12} - C_{12}(C_{23} + C_{12}) - C_{13}(C_{12} + C_{13}) - C_{23}(C_{13} + C_{23})] / \Delta + 3[(1/C_{44}) + (1/C_{55}) + (1/C_{66})] \}^{-1},$$

where  $\Delta = C_{13}(C_{12}C_{23} - C_{13}C_{22}) + C_{23}(C_{12}C_{13} - C_{23}C_{11}) + C_{33}(C_{11}C_{22} - C_{12}^2)$ .

The shear modulus and bulk modulus are derived from the Voigt-Reuss-Hill average value. In terms of the Voigt-Reuss-Hill approximations [41], the shear modulus G and bulk modulus B are expressed as,  $G = (G_R + G_V)/2$  and  $B = (B_R + B_V)/2$  with Young's modulus,  $E = 9BG/(3B + G)$ . The shear strengths are related to the plastic deformation and obtained from stress-strain curve. The stress-strain curve along a direction in some planes was obtained by straining the structure with the way of step-by-step from

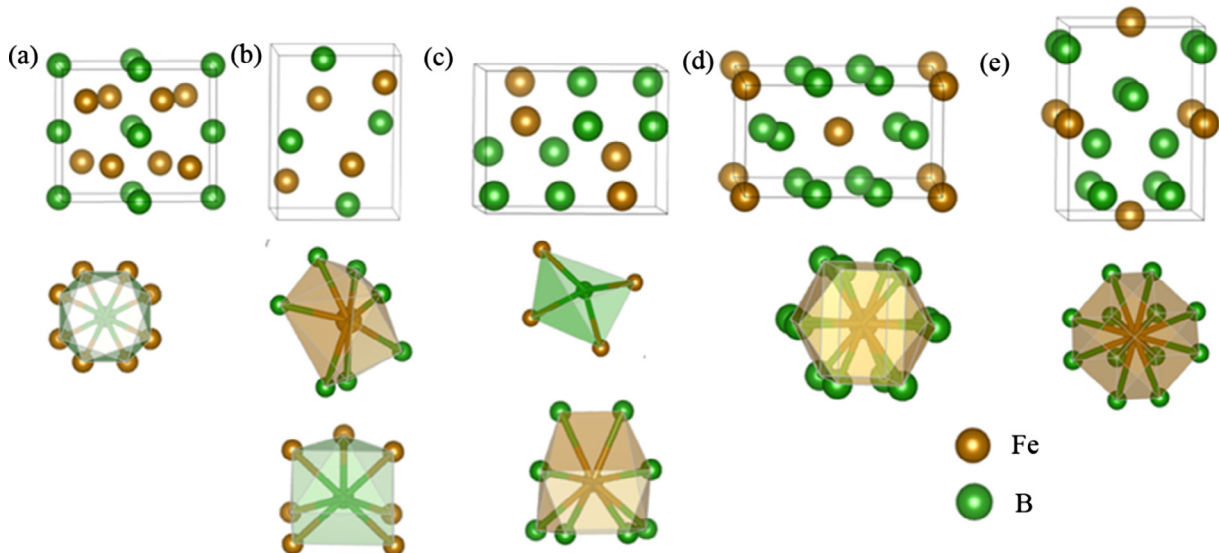


Fig. 1. Crystal structures and coordination numbers for different single-phase structures of FeB<sub>x</sub> including Fe<sub>2</sub>B (a), FeB (b), FeB<sub>2</sub> (c), ambient pressure phase FeB<sub>4</sub> (op10-FeB<sub>4</sub>) (d) and high pressure phase FeB<sub>4</sub> (tp10-FeB<sub>4</sub>) (e).

Download English Version:

<https://daneshyari.com/en/article/7958183>

Download Persian Version:

<https://daneshyari.com/article/7958183>

[Daneshyari.com](https://daneshyari.com)